Applied Energy xxx (2016) xxx–xxx

Contents lists available at ScienceDirect

Applied Energy

journal homepage: www.elsevier.com/locate/apenergy

Coupling Solid Oxide Electrolyser (SOE) and ammonia production plant

Giovanni Cinti [a,*], Domenico Frattini [b], Elio Jannelli [b], Umberto Desideri [c], Gianni Bidini [a]

[a] Università degli Studi di Perugia, via Duranti 93, 06125 Perugia, Italy
[b] Università degli Studi di Napoli Parthenope, Centro Direzionale Napoli Isola C4, 80143 Naples, Italy
[c] Università degli Studi di Pisa, Largo Lucio Lazzarino, 56122 Pisa, Italy

HIGHLIGHTS

- An innovative NH_3 production plant was designed.
- CO_2 emissions and energy consumption are studied in three different designs.
- High temperature electrolysis allows to achieve high efficiency and heat recovery.
- The coupling permits storage of electricity into a liquid carbon free chemical.

ARTICLE INFO

Article history:
Received 14 April 2016
Received in revised form 7 September 2016
Accepted 9 September 2016
Available online xxxx

Keywords:
Sustainable ammonia synthesis
Energy storage
Solid Oxide Electrolyser

ABSTRACT

Ammonia is one of the most produced chemicals worldwide and is currently synthesized using nitrogen separated from air and hydrogen from natural gas reforming with consequent high consumption of fossil fuel and high emission of CO_2. A renewable path for ammonia production is desirable considering the potential development of ammonia as energy carrier. This study reports design and analysis of an innovative system for the production of green ammonia using electricity from renewable energy sources. This concept couples Solid Oxide Electrolysis (SOE), for the production of hydrogen, with an improved Haber Bosch Reactor (HBR), for ammonia synthesis. An air separator is also introduced to supply pure nitrogen. SOE operates with extremely high efficiency recovering high temperature heat from the Haber-Bosch reactor. Aspen was used to develop a model to study the performance of the plant. Both the SOE and the HBR operate at 650 °C. Ammonia production with zero emission of CO_2 can be obtained with a reduction of 40% of power input compared to equivalent plants.

1. Introduction

Ammonia was presented recently as a potential fuel and as an eligible energy vector [1]. Such opportunity comes from ammonia high energy density. Volumetric and gravimetric energy density of ammonia at room temperature and 10 bar are 22.5 MJ/kg and 13.6 GJ/m^3 respectively, higher than other candidates such as hydrogen and methanol and not far from fossil sources such as gasoline, diesel and compressed natural gas. The utilization of ammonia as a fuel was reported with interesting results in traditional power units [2,3]. Ammonia combustion releases heat that can be used in both internal and external combustion engines [4]. In addition, the use of ammonia as a fuel is also demonstrated in fuel cells with consequent advantages in terms of low emissions and high efficiency. Ammonia is a carbon free fuel, no CO_2 is emitted when burnt, and in fuel cell applications the risk of NO_x emissions is reduced because no direct mix between oxygen and ammonia occurs. A sustainable use of ammonia both as a chemical and as a fuel requires a renewable production of nitrogen and hydrogen [5,6]. Ammonia is usually produced in the Haber-Bosch (HB) loop reactor from pure hydrogen and nitrogen that are fed and recirculated in the reactor, operating at high pressure and high temperature. Hydrogen is commercially produced from fossil sources, such as natural gas, normally in an autothermal steam methane reformer or in a steam methane reformer, while nitrogen is separated from air. In order to call ammonia a green chemical, both hydrogen and nitrogen should be produced and supplied using renewable energy as a primary source: biomass [7], wind [8] or solar energy [9] can guarantee a renewable and sustainable production of ammonia based on thermochemical or electrochemical processes [10]. In particular, from water electrolysis and air separation powered by renewable electricity it is possible to produce green ammonia without any CO_2 emission to the atmosphere [11].

* Corresponding author.
E-mail address: giovanni.cinti@unipg.it (G. Cinti).

http://dx.doi.org/10.1016/j.apenergy.2016.09.026
0306-2619/

This kind of plant can also be used in electric grids with a large penetration of intermittent renewable energy sources to store energy into a liquid fuel that allows the spatial and temporal separation, of energy supply and demand. The green ammonia plant allows to store directly the renewable electricity into a chemical with high energy density, quite easy to stock and to transport. This concept was recently presented and studied in the literature [12,13]. An additional advantage of the proposed concept is that compared to the storage of renewable electricity into fuels such as methane, methanol or synthetic diesel; ammonia production does not require carbon dioxide but nitrogen as additional gas input. Both nitrogen and carbon dioxide can be separated from the air but the higher concentration of nitrogen increases efficiency and lowers production cost in comparison with CO_2.

Recent developments of Solid Oxide Fuel Cells (SOFCs) renewed interest in high temperature Solid Oxide Electrolysers (SOEs), based on the same materials and design [14]. SOEs operate with higher power density and higher efficiency compared to traditional electrolysers, especially if fed with high temperature waste heat, because the electrochemical conversion of water at high temperatures opens the opportunity to store both heat and electricity in the produced hydrogen [15]. Such opportunity is currently under study in industrial processes where waste heat recovery at high temperature is available. For example, coupling is possible with nuclear power plants where heat is usually a by-product [16], or with solar collectors in solar thermal power plants, where renewable heat comes from the sun [17] in order to achieve energy storage or production of secondary fuels or energy vectors [18]. In this scenario, the coupling of SOE and HB process is extremely interesting. NH_3 synthesis is an exothermal chemical reaction at high temperature and pressure, producing a large amount of heat. The integration between the HB process and the SOE potentially allows to transfer the heat produced by the HB reactor to the SOE to increase its performance. Moreover, the feasibility of ammonia production from renewable energy via electrolysis of water is very important to produce sustainable fuels and chemicals.

This study proposes an improvement to green ammonia production plants introducing, for the first time, an SOE for H_2 production in a HB process. In addition to the studies already cited above literature reports, for example, system designs based on wind power with a small efficiency and a limited degree of integration [19]. The new concept proposed in this work permits system implementation and allows to improve the power to ammonia storage efficiency. An electrochemical model and a thermodynamic simulation of a system layout, in which an SOE and an NH_3 plant are integrated and operated at high pressure and temperature, has been developed to evaluate the potential of the proposed concept with respect to other green solutions and to a reference benchmark case, based on the use of natural gas. The effect on the global efficiency and on avoided CO_2 emissions is evaluated. This work can enhance the development of green ammonia and can offer, at the same time, an interesting application of SOE, pushing the development and application of the technology not only in the energy sector but also in the chemicals production field. In the following paragraphs the theory and modelling of SOE and HB process are presented, the design of the model is described and, finally, the main results are analysed and commented.

2. Theoretical background and model development

2.1. Considerations for coupling and SOE electrochemical model

Ammonia synthesis is realized mainly with the plant design developed by Haber and Bosch (HB). The HB process considered in this work is based on a modern layout, as shown in Fig. 1.

Ammonia synthesis is an exothermal process based on the following chemical reaction:

$$\frac{3}{2}H_2 + \frac{1}{2}N_2 \leftrightarrow NH_3 \quad \Delta H^\circ = -45.7\ \text{kJ/mol}\ H_2 \tag{1}$$

The distinctive physical aspects of this equilibrium reaction is the contrasting effect of pressure and temperature on thermodynamics and kinetics, according to the following equation [20]:

$$K_{NH_3} = K_\varphi \cdot K_p = \left(\frac{\varphi_{NH_3}}{\varphi_{N_2}^{1/2} \cdot \varphi_{H_2}^{3/2}}\right) \cdot \left(\frac{n_{NH_3}}{n_{N_2}^{1/2} \cdot n_{H_2}^{3/2}} \cdot \frac{n_{tot}}{P_{tot}}\right) \tag{2}$$

The left hand side is the chemical equilibrium constant in which non ideal fugacity coefficients are accounted in the term K_φ. The term K_p account for the reactor operating conditions, especially the presence of inert species, which can decrease the molar fraction of reactants and so the production of ammonia. On the other hand, as the total pressure increases, also the conversion of reagents into ammonia increases. The reaction kinetic is governed by the Temkin-Pyzhev equations [21] in which the reaction rate of the reverse process is negligible as the reactor temperature increases, but, due to the exothermal characteristic of the thermodynamic equilibrium, the chemical equilibrium constant is lower. Ammonia synthesis is realized mainly with the plant design developed by Haber and Bosch (HB). The HB process considered in this work is based on a modern layout, as shown in Fig. 1. The main features, according to the above thermodynamic and kinetic considerations, are the recycle streams, two stages of ammonia separation (before and after each reactor passage) and heat recovery from products to increase productivity and reduce energy requirements. As a consequence, an efficient and high conversion of reactants in the HB reactor is favored by:

- High pressure and temperature of the reactor.
- Stoichiometric H_2/N_2 ratio in the reactor feeding stream.
- Absence of inerts or diluting species.
- Auxiliary streams for purging inerts and for recirculation of unconverted gasses.

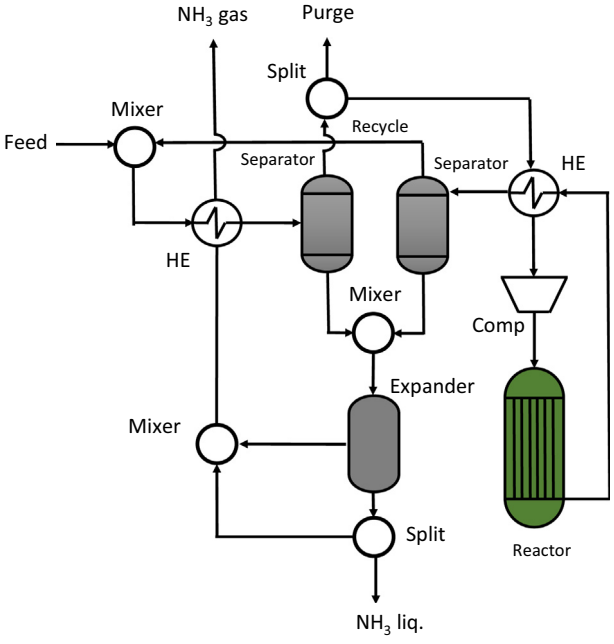

Fig. 1. HB process layout for production of NH_3.

From the physical point of view, the first two points determine the conversion per single pass in the HB reactor and, according to thermodynamics, an isothermal reactor should be preferred, with an efficient reaction heat recovery system, which is the major source of waste heat. The last two points mainly contribute to the global conversion and productivity of the plant. In fact, a feeding stream with a low content of inerts limits the need to partially purge unreacted gases, reduces the hydrogen losses in the tail gas, increases the recycle ratio in the HB loop as more ammonia can be produced and separated at each pass and the global conversion efficiency increases. Other relevant processes that affect the HB plant are syngas production and purification. Steam Methane Reforming (SMR) and Water Gas Shift (WGS) are the main processes involved in syngas production while physical and chemical separation processes, based on condensation, membranes and absorption at low temperatures, are used to purify syngas from species such as H_2O, CO, CO_2 and CH_4 [22]. On the other hand, electricity-based processes for H_2/N_2 production, such as electrolysis, cryogenic air separation and Pressure Swing Adsorption (PSA) [23] can be considered for syngas production as they involve low temperatures and mild thermodynamic conditions. So, from the thermodynamic point of view, exothermal and endothermal processes are simultaneously involved and, considering the presence of high and low temperature units, heat recovery issues arise in order to optimize the system design and process integration as these aspects influence the energy efficiency and the production of the overall plant. In this background, it is clear that a proper integration between different technologies to improve the HB process requires an overall system evaluation in order to verify benefits and drawbacks of each solution.

SOE conceptual scheme is depicted in Fig. 2.

Anodic and cathodic reactions are:

$$\text{Anode} \quad O^{2-} \rightarrow 2e^- + \frac{1}{2}O_2 \tag{3}$$

$$\text{Cathode} \quad H_2O + 2e^- \rightarrow H_2 + O^{2-} \tag{4}$$

The overall electrolysis reaction is the following:

$$H_2O \leftrightarrow H_2 + \frac{1}{2}O_2 \tag{5}$$

The reaction is endothermal and the enthalpy change has to be supplied externally. In electrochemical devices, such as fuel cells, energy is supplied as electrical (ΔG) and thermal energy ($T\Delta S$). Thermal energy is usually generated inside the cell, recovering heat from internal polarization losses. With the increase of temperature, total energy requirement (ΔH) increases but the amount of electrical energy is smaller. The result is a higher efficiency of the high temperature electrolyser than the low temperature ones. If part of the necessary heat is supplied by an external source, it is possible to achieve higher than one efficiency, obtaining the conversion of thermal energy into chemicals.

Thermodynamic values at 650 °C are reported in Table 1. Note that values are normalized for one mole of H_2 produced (electrolysis) or reacting (ammonia synthesis).

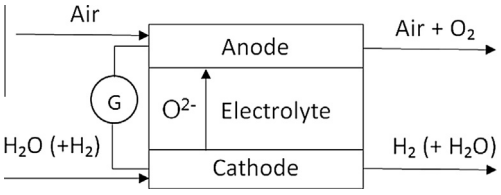

Fig. 2. SOE conceptual scheme.

Ammonia synthesis can supply up to 98% (39.14 kJ/mol H_2) of the heat required, in terms of entropy, of the electrolysis reaction (39.66 kJ/mol H_2). In order to couple thermodynamic and electrochemical calculations for integration with the HB process, a zero dimension model for the SOE was developed as follows.

In an SOE, the electrical inputs creates the electron flows involved in the reactions. In electrolysers, voltage is a function of current density and can be described with a very simple linear law as follows:

$$V = OCV + ASR(T) * J \tag{6}$$

Were OCV is the Open Circuit Voltage, ASR is Area Specific Resistance and J is current density. Both OCV and ASR are function of temperature. This simplified approach is supported by experimental results that show how the polarization curve is highly linear at high temperature [24]. In additions authors already demonstrated how ASR does not change between SOFC and SOE operation [25]. This assumption will be used in defining values of ASR. In the following equation (iv) SOE electrical power density is described as follows:

$$P_e = V * J = OCVJ + ASR * J^2 \tag{7}$$

Energy output of the SOE is the energy of produced hydrogen. Such energy is the chemical energy of the fuel usually quantified in the LHV. For this study such energy was considered the enthalpy of the reaction (1) equivalent to the LHV of the fuel. Differently from LHV, the calculation was performed at the operational temperature. Specific chemical energy (in terms of energy flow per unit area) converted in the SOE is defined as follows:

$$\Delta H = dh(T) * H_{2mol} \tag{8}$$

where H_{2mol} is the specific molar flow (mol/m^2) of hydrogen and dh (T) is the enthalpy of the reaction (1). Hydrogen specific flow and current density are connected to the electrochemical parameters by the equation:

$$H_{2mol} = \frac{J}{2 * F} \tag{9}$$

where F is the Faraday constant. Differently from fuel cells, the chemical reaction in electrolysers is endothermal and the heat losses of the process, such as overpotential losses, are in equilibrium with reaction requirements. The energy balance is completed by the contribution of heat transfer with the external source. The latter takes into account the SOE heat losses into the environment and the heat inlet from the environment that may come from a high temperature heat source, as in this application. External heat (Q) is calculated, for the present study, as a function of hydrogen energy production by the following equation

$$Q = k * \Delta H \tag{10}$$

The energy balance of the SOE is defined by the following equation:

$$P_e = \Delta H + Q = \Delta H(1 + k) \tag{11}$$

Differently from fuel cells, were produced heat has to be subtracted by the air flow, in SOEs the external heat contribution plays an important role not only on the operational temperature but also on the performance. Assuming the stack at constant temperature, Eq. (12) directly relates current density and temperature to the external heat. Thus, temperature definition and k allow to calculate the current density. Considering the previous equations J can be calculated as:

$$J = \frac{1}{ASR}\left(\frac{dh(T) * (1 + k)}{2 * F} - OCV\right) \tag{12}$$

Efficiency is calculated as the ration between energy output (ΔH) and energy input (P_e) by the following equation:

Please cite this article in press as: Cinti G et al. Coupling Solid Oxide Electrolyser (SOE) and ammonia production plant. Appl Energy (2016), http://dx.doi.org/10.1016/j.apenergy.2016.09.026

Table 1
Thermodynamic values of involved reactions.

	Temperature [°C]	Pressure [bar]	ΔH [kJ/mol H_2]	TΔS [kJ/mol H_2]	ΔG [kJ/mol H_2]
Water electrolysis	650	1	247.32	39.66	207.65
Ammonia synthesis	650	550	−39.14	−83.68	44.54

$$\eta = \frac{\Delta H}{P_e} = \frac{1}{1+k} \tag{13}$$

Note that the efficiency is only a function of external heat contribution (k). In the specific case of k = 0 the SOE operates in adiabatic conditions (no heat exchange with the environment) with a 100% theoretical efficiency. This operational condition is called thermoneutral. All equations were implemented in a zero-dimensional model developed using Excel and FluidProp© as cathode for thermodynamic parameters. The OCV value was calculated using the well-known Nernst equation considering at cathode inlet a steam flow with 10% hydrogen (necessary for the integrity of the electrode) and at anode inlet air. ASR values are derived from a SOFC commercial product [17] due to the aforementioned equivalence with SOE ones.

2.2. Description of developed case studies

In order to assess the profitability of coupling SOE and HB process for the production of green ammonia, Process Flow Diagrams (PFDs) were realized in the AspenPlus environment to compare different scenarios. In particular, three case studies were developed. A brief description of the relevant process physics of each developed layout is given below. More details about the flowsheets and the specific parameters used to model the single blocks in AspenPlus are given in Appendix A. Considering the high temperature and high pressure conditions for the HB loop, no kinetic approaches are applied for simulations and only the thermodynamic equilibrium is considered.

The plant layout for the reference case, named NG-REF-HB, with conventional NH_3 production from natural gas is shown in Fig. 3.

In this plant the upstream process is the CH_4 steam reforming, where many units are required for the clean-up of the reformed gas in order to obtain a feed stream for the ammonia production with the appropriate composition. In fact, the reforming process is endothermal and requires a large amount of heat. The first burner is adiabatic and the amount of oxygen introduced is not sufficient to oxidize all the fuel and a partial gasification occurs with H_2 and CO formed together with CO_2 with the aim to partially provide the necessary heat for reforming and H_2 for the synthesis. In the subsequent WGS section, CO reacts with steam to produce H_2, thus increasing hydrogen content in the syngas for ammonia production. The Acid Gas Removal unit (AGR), the Methanator unit (METH) and the Condenser (COND) are devoted to the physical and chemical separation and removal of CO_2, CO and H_2O after the WGS section. These processes require a much lower temperature (50–100 °C) than that of WGS (250–550 °C). The waste heat available is recovered to produce the high temperature steam for the reforming unit. From the thermodynamic point of view, the operating conditions of these units must be accurately chosen in order to correctly simulate the physics of the process.

In Fig. 4 the low temperature electrolysis case, named EL-PSA-HB, with H_2 produced from commercial electrolysers and N_2 produced by PSA, is shown.

This layout is completely different from the previous one. The feeding streams to the plant are air and water, at ambient condition, as primary sources for H_2 and N_2. From the physical point of view, the principal characteristic of this solution is that no chemical energy, as fuel, is introduced and the only energy input is electricity, thus the thermodynamic of the process does not involve high temperatures, pressures or large heat exchangers. In agreement with the actual water electrolysers performance, a hydrogen purity of 99.9% and an electrical efficiency of 64.4% have been specified for this block [26]. The air separation unit is based on a PSA standard process at room temperature and 30 bar, with commercial carbon molecular sieves as adsorbent [27].

Finally, the case of SOE and HB with heat recovery from the synthesis reactor, SOE-PSA-HB, is shown in Fig. 5.

From the thermodynamic point of view, the main difference with the previous case is that the low temperature electrolysis is replaced by the high temperature one. The physics of the upstream section, representing the SOE unit, has been already discussed in previous works [28] and slightly modified as specified in Appendix A. Briefly, the main modifications for thermodynamic reasons concern the operating temperature and the thermal input of SOE that matches the conditions imposed by the HB reactor. This ties the coupling task to the energy balance and thermodynamic equilibrium of the overall system.

3. Results and discussion

Fig. 6 reports the variation of hydrogen production rate and efficiency (a) and of electrical power input and voltage (b) as a function of temperature for three values of k: k = 0 (thermoneutral), k = 0.2 (heat into the SOE) and k = −0.2 (heat losses). Fig. 6a shows a trade-off between efficiency and hydrogen production: with higher values of k smaller efficiency can be obtained. As expected from Eq. (13), efficiency is not affected by temperature variation while hydrogen production increases with temperature due to the decrease of internal resistances (ASR). Regarding Fig. 6b, the electrical power density increases with temperature and is higher when k is smaller (heat losses). Cell voltage remains constant at current density variation while it increases when k decreases. Thermoneutral voltage obtained is approximately 1.29 V in agreement with the literature [14].

Considering the coupling of ammonia synthesis with SOE, it is possible to calculate the k factor, considering the heat flow from the ammonia reactor calculated from the Aspen model. At the operating temperature of 650 °C all other SOE parameters are calculated and reported in Table 2.

In order to compare the performance of the different cases considered, the following Table 3 shows the major comparative parameters for the three scenarios. They refer only to the HB loop subsection of the flowsheets.

The global efficiency η_{glob} is based on the overall H_2 molar balance around the flowsheet as it takes into consideration the chemical conversion of hydrogen and also the separation of the unreacted moles for the internal recycle. On the other hand, the reactor efficiency η_{react} represents the conversion of H_2 per pass on molar basis inside the block REACTOR as it depends on the inlet molar composition and the operating condition of the HB loop. Comparing the values, remarkable differences are visible between the reference case, i.e. NG-REF-HB, and the remaining two, while the results obtained for the two cases with the use of electrolysers seem to be very similar. The first two plants, the first fed with natural gas and the second based on a low temperature standard electrolyser, can be operated at middle HB reactor conditions (250 bar

Please cite this article in press as: Cinti G et al. Coupling Solid Oxide Electrolyser (SOE) and ammonia production plant. Appl Energy (2016), http://dx.doi.org/10.1016/j.apenergy.2016.09.026

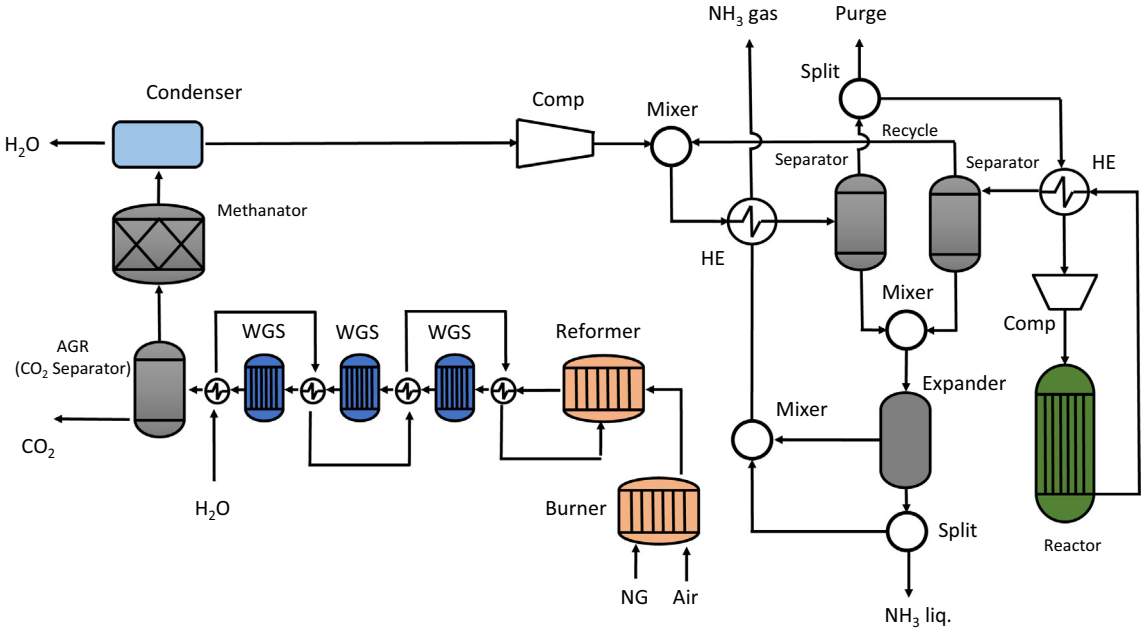

Fig. 3. Layout of the reference case NG-REF-HB.

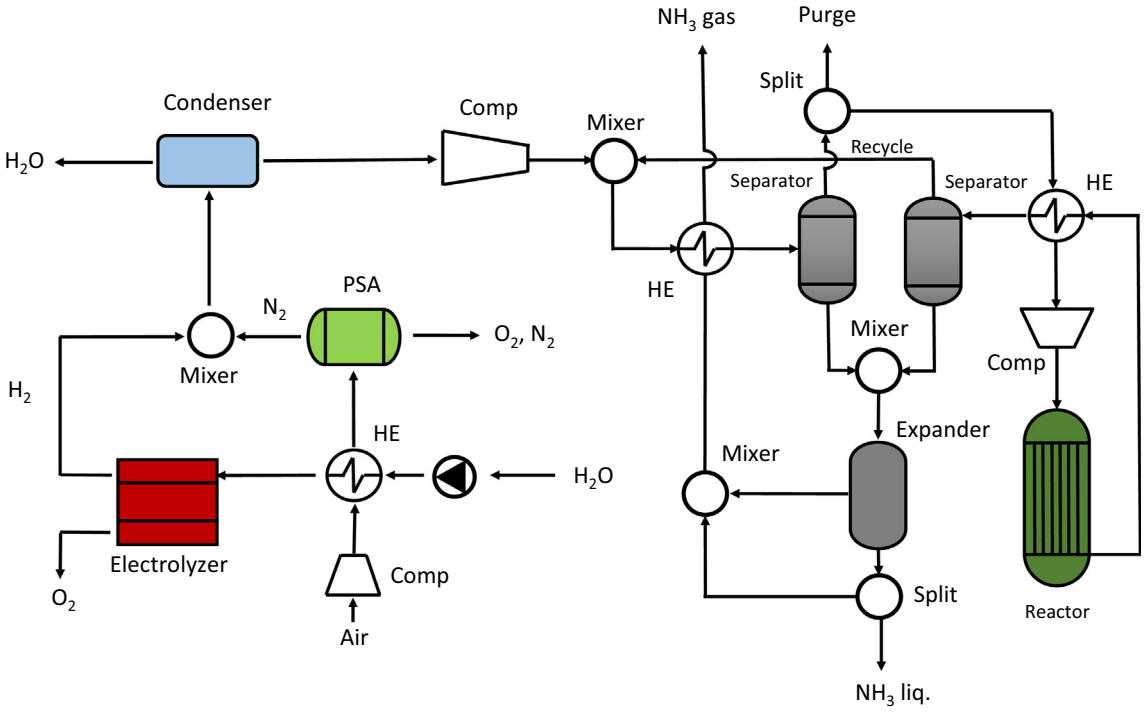

Fig. 4. Layout of the low temperature electrolysis case EL-PSA-HB.

and 550 °C). SOE necessarily requires heavy HB reactor conditions (550 bar and 650 °C) for coupling, as discussed in Section 2.1. Contrarily to what could be expected, the conversion per pass and the global efficiency is very different for NG-REF-HB and EL-PSA-HB, even if temperature and pressure of the HB reactor are the same. This is due to the high content of inerts in the reference case, i.e. CH_4, that dilutes the reactant steam and affects negatively the K_p term as envisaged from Eq. (2). Moreover, the dilution of the products by CH_4 affects the physical separation of ammonia because it reduces the partial pressure of NH_3 in SEP01 and SEP02 blocks. This is the cause of the low η_{glob} and the deviation of the H_2/N_2 ratio inside the HB loop. As a consequence, the resulting purge ratio, i.e. the purge gas stream, should be higher in order to avoid the accumulation of inerts in the loop. On the contrary, the two cases with electrolysers have very similar HB loop performances due to the complete absence of inerts. This is a distinguishing feature of ammonia production when electrolysis and air separation are used to provide the H_2/N_2 mixture. In particular, the purge ratio is very

Please cite this article in press as: Cinti G et al. Coupling Solid Oxide Electrolyser (SOE) and ammonia production plant. Appl Energy (2016), http://dx.doi.org/10.1016/j.apenergy.2016.09.026

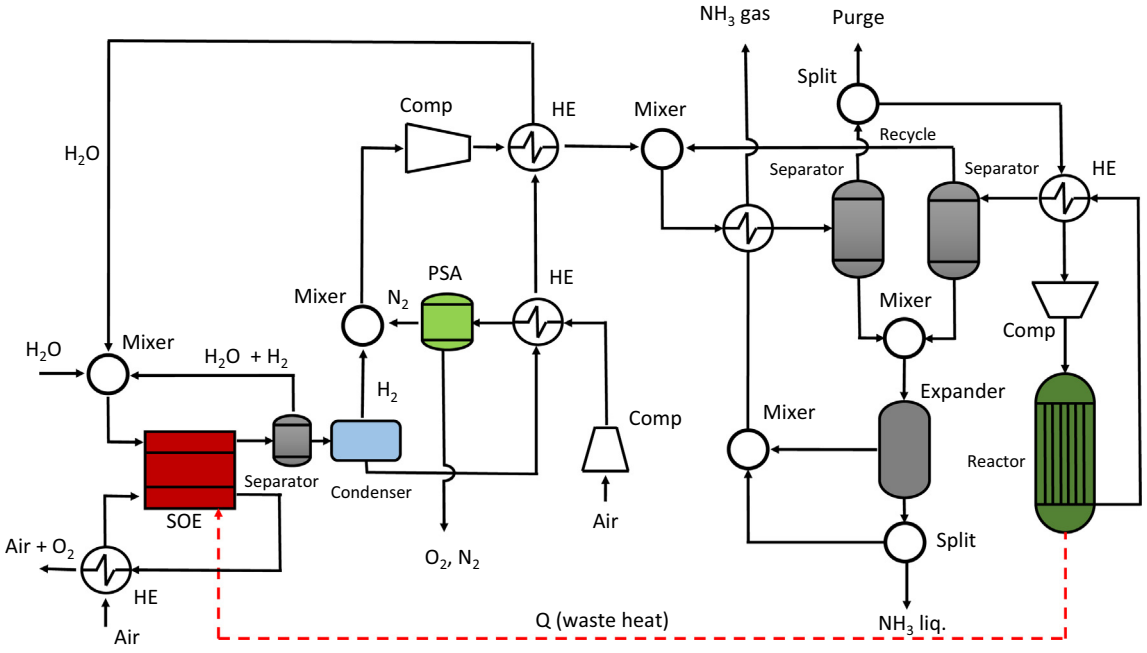

Fig. 5. Layout of the high temperature electrolysis case SOE-PSA-HB.

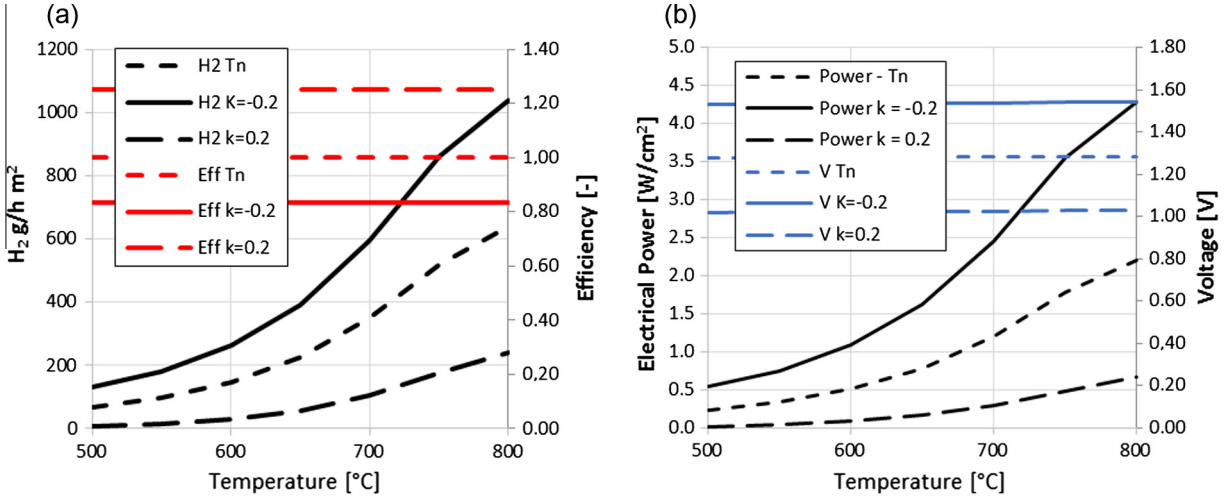

Fig. 6. Effect of temperature and k (a) hydrogen production rate and efficiency; (b) electrical power and voltage.

Table 2
SOE parameter when integrated with NH_3 synthesis.

Parameter	Units	Value
k	–	0.15
Temperature	°C	650
ASR	Ω·cm^2	0.57
OCV	V	0.94
H_2	g/h·m^2	102.56
J	A/cm^2	0.27
Voltage	V	1.09
Power density	W/cm^2	0.35
η	–	1.17

small, so that more reactants can be recycled to the reactor instead of being purged with inerts. As a consequence, the recycle ratio, the NH_3 produced and the global efficiency increase.

In Table 4 the overall energy consumptions and the equivalent Greenhouse Gas (GHG) emissions of the three cases are reported. The equations used for calculations are the following:

$$Spec.Chem.Cons. = \frac{\sum \dot{n}_i \cdot LHV_i}{\dot{m}^{TOT}_{NH3}} \quad (14)$$

$$Spec.Elec.Cons. = \frac{\sum P^{el}_j}{\dot{m}^{TOT}_{NH3}} \quad (15)$$

$$Spec.Heat\,Cons. = \frac{\sum P^{th}_j}{\dot{m}^{TOT}_{NH3}} \quad (16)$$

$$GHG\ Emissions = \frac{(\dot{n}_{CO} + \dot{n}_{CO2} + \dot{n}_{CH4}) \cdot M_{CO2}}{\dot{m}^{TOT}_{NH3}} \quad (17)$$

Table 3
HB loop performances for the three different case studies.

	$(H_2/N_2)_{FEED}$ (mol/mol)	$(H_2/N_2)_{IN}$ (mol/mol)	Rec. ratio (mol/mol)	Purge ratio (mol/mol)	LHV_{PURGE} (MJ/kg)	η_{glob} (%)	η_{react} (%)
NG-REF-HB	3.07	3.17	3.33	0.44	26.76	61.12	18.25
EL-PSA-HB	3.01	3.02	4.29	0.08	21.35	92.33	21.06
SOE-PSA-HB	3.00	3.03	4.30	0.06	21.43	93.40	19.53

Table 4
Energy performances for the three different case studies.

	Spec. chem. cons. (kW h/kg_{NH3})	Spec. elec. cons. (kW h_{el}/kg_{NH3})	Spec. tot. cons. (kW h/kg_{NH3})	Spec. heat cons. (kW h_{th}/kg_{NH3})	GHG emissions (kg_{CO2eq}/kg_{NH3})	Storage eff. (%)
NG-REF-HB	12.81	1.77	14.59	−1.20	2.05	35.50
EL-PSA-HB	0	14.25	14.25	−1.63	0	36.35
SOE-PSA-HB	0	8.30	8.30	−1.14	0	62.41

$$Storage\,Eff. = \frac{\dot{m}^{TOT}_{NH3} \cdot LHV_{NH3}}{\sum \dot{n}_i \cdot LHV_i + \sum P^{el}_j} \cdot 100 \quad (18)$$

where $\sum \dot{n}_i \cdot LHV_i$ is the total chemical energy entering the flowsheet, $\sum P^{el}_j$ is the sum of all the electric power and $\sum P^{th}_j$ is the sum of all the heat flux of the generic block j in the flowsheet. The specific total consumption is the sum of the values calculated from Eqs. (14) and (15). They are all normalized on $\dot{m}^{TOT}_{NH3}$, i.e. the total quantity of ammonia produced, considering both liquid and gaseous ammonia in output streams. As reference, positive values are intended as energy provided to the system, while negative values represent energy that should be subtracted from the system.

The first evident results is that for the case EL-PSA-HB and SOE-PSA-HB the specific chemical consumption is zero: these systems are fed only by air and water so that there is no energy cost. On the contrary, the NG-REF-HB uses a fuel, i.e. CH_4, as feedstock. As expected, only the first case has a net environmental impact in terms of GHG emissions due to the CO_2 release during the reforming and clean-up operations of the fuel. This is mainly concentrated in the AGR block of the flowsheet in Fig. 3, because it is one of the units devoted to the removal of oxygenated species from the syngas for NH_3 synthesis. The remaining two cases have no net emissions because their feedstock is "carbon-free". The purge gas of the NG-REF-HB contains CH_4, which is a greenhouse gas, but the emission related to this gas is not accounted to the plant due to the fact that this stream can be stored as a secondary fuel or as a chemical feedstock for other purposes. Moreover, keeping in mind the previous purge ratios and global efficiencies, it can be concluded that the quantity of purge gas produced is considerable in the first system but negligible in the other two. Finally, a significant difference on the total and heat consumptions occurs in all cases. In particular, even though the HB loop performances are quite the same, the cases with electrolyser have very different consumptions. Comparing the reference case and the standard electrolyser case, it is worth to observe that the total consumption is not so different, so that there is a little benefit in preferring the electrolysis pathway, power-intensive but low impacting, rather than the traditional one, based on fossil fuel and less electricity-consuming with the perspective to produce a valuable tail gas. However, the

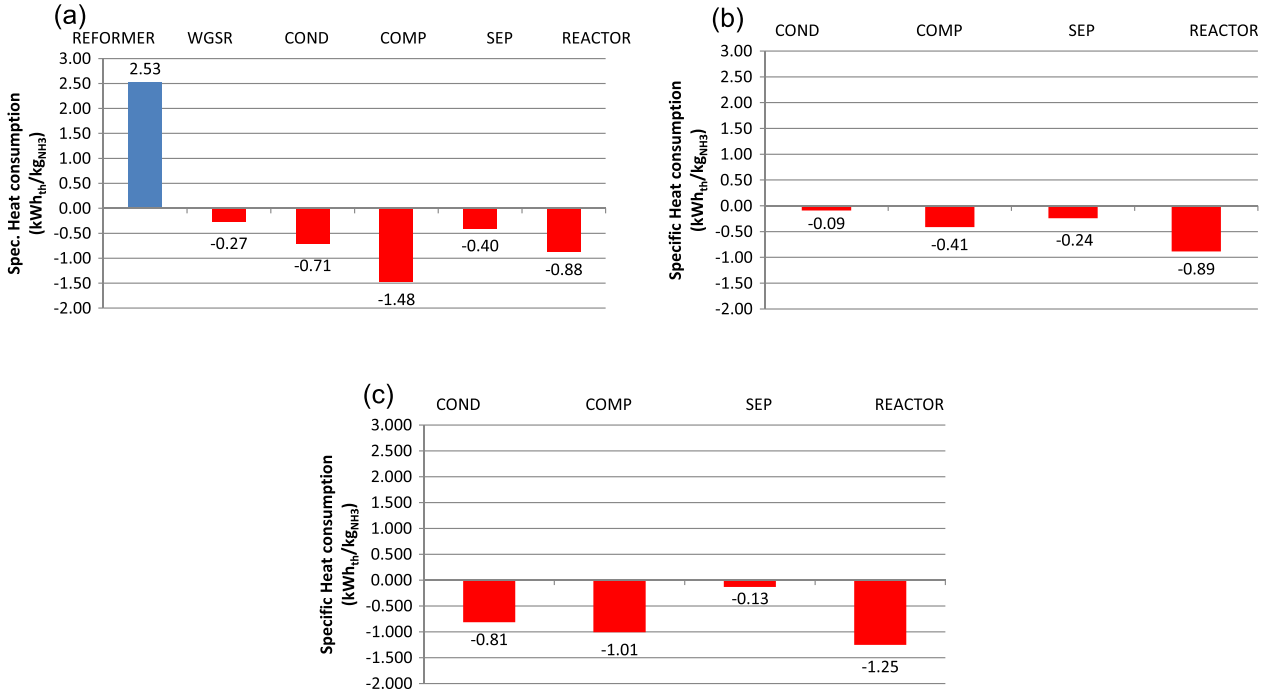

Fig. 7. Specific heat consumption of ancillaries: (a) NG-REF-HB; (b) EL-PSA-HB; (c) SOE-PSA-HB.

Please cite this article in press as: Cinti G et al. Coupling Solid Oxide Electrolyser (SOE) and ammonia production plant. Appl Energy (2016), http://dx.doi.org/10.1016/j.apenergy.2016.09.026

results show that in the case of coupling SOE, PSA and HB, the total energy consumption can be potentially lower than all other proposed solutions. In addition, considering the perspective of the storage of electricity into a chemical vector, i.e. NH_3, the calculation shows that the SOE-HB coupling has a potential storage efficiency of 62.4% and that it is almost two times higher than EL-PSA-HB and NG-REF-HB cases. The advantage of using high efficiency and high temperature electrolysis in a SOE is thus evident and integrated in a conventional chemical process like ammonia production.

To better understand this, in Fig. 7, the detailed consumption of heat is specified for the main ancillaries of the three developed scenarios. For the reference case, which has more ancillaries than the other cases, there is a considerable endothermal term, due to the heat required by the reformer block, and a higher exothermal contribution from the compression units, due to the intercooling.

The other two cases have smaller contributions, due to the simpler layout with no fuel thermal treatments or gas clean-up units. Comparing Figs. 7a and b, the heat available from HB reactor is the same because the operating conditions are the same but, due to the presence of a large amount of inerts, the amount of heat that should be removed from COMP is larger. The presence of species other than H_2, N_2 and NH_3 in the HB loop is a strong limit for productivity but also energy efficiency of traditional HB plant because, if compared to the contribution of an electrolysis-based plant, they cause lower conversion and larger amounts of waste heat. From this point of view, the SOE-PSA-HB offers more flexibility and opportunity for a convenient recovery of waste heat. In Fig. 7c not all the contributions reported are really lost because, as shown by the flowsheet of Fig. A4 in appendix, the heat from COND and REACTOR are used to achieve the thermal equilibrium of the SOE block because this acts as a "heat sink" for the system. In detail, the heat from REACTOR is entirely used to feed SOE and is an input for the design of the electrolyser. Compared to low temperature electrolysis steam is supplied to SOE instead of water. The amount of energy to vaporize water, 1.79 kW h/kg_{NH3} can be recovered partially from the compressor, where 1.01 kW h/kg_{NH3} are released from intercoolers, and from condenser, where 0.81 kW h/kg_{NH3} are released at high temperature. An additional advantage of this configuration is that no cooling of ammonia reactor is required reducing the environmental impact in terms of plant waste heat. One of the actual issue for SOE is that it requires a large amount of heat, or a high current density, from external sources to sustain the high temperature electrolysis process. If SOE and HB loop can be operated at similar temperatures, their coupling offer the opportunity to recover the large amount of heat available from HB reactor to achieve a stable thermal equilibrium in the SOE, without increasing the current density, i.e. the electricity consumption, as explained in the model above. The single contributions of COND and REACTOR in the SOE-PSA-HB case are reported for completeness and to show how they become of interest if compared to that of the mild HB reactor conditions.

The direct consequence of this fact can be immediately realized if the single electric consumptions are compared as shown in Fig. 8.

The first two columns clearly show the advantage of the high temperature electrolysis over the low temperature one, if additional heat is provided from another source. The consumptions related to the PSA subsection are the same for both cases, as expected, while the electric consumptions related to the compression units of the HB loop are very different, essentially due to the high pressure imposed at the REACTOR block of the SOE-PSA-HB. It is worth noting that for the reference case the electric consumption is represented only by the compression units in the HB loop, and that its value is 1.77 kW h/kg_{NH3}, the highest among the three scenarios, because a large part of this energy is used to compress inerts which dilutes the syngas stream.

The coupling of SOE and HB deeply affects the energy balance of the plant when the electrolysis is used in place of the reforming of a fossil fuel. Moreover, the type of electrolysis process modifies the distribution of energy consumption within the plant itself. The situation is briefly explained in Fig. 9.

When a low temperature electrolysis is used to produce the syngas for the HB loop, the electric consumption related to the electrolyser operation is >95% of the total, i.e. the overall energy balance is in practice restricted to the electrolyser, so that there is no flexibility and the whole plant is dependent from the electrol-

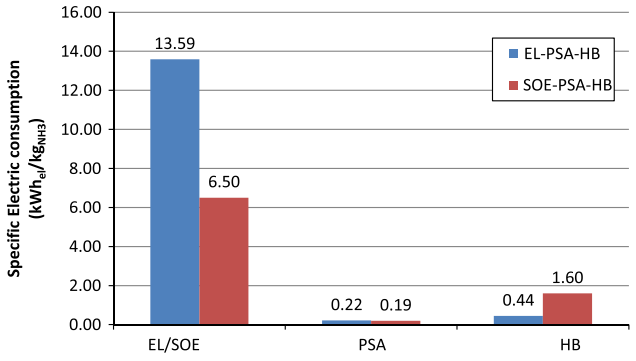

Fig. 8. Comparison of the electric consumption for EL-PSA-HB and SOE-PSA-HB cases.

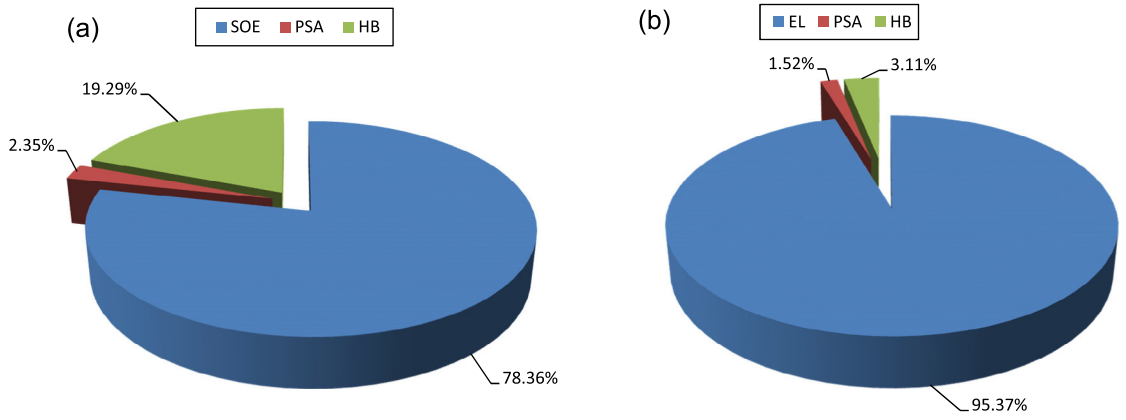

Fig. 9. Distribution of the specific electric consumption: (a) EL-PSA-HB; (b) SOE-PSA-HB.

Please cite this article in press as: Cinti G et al. Coupling Solid Oxide Electrolyser (SOE) and ammonia production plant. Appl Energy (2016), http://dx.doi.org/10.1016/j.apenergy.2016.09.026

ysis subsection. On the other hand, when a SOE is implemented, its impact on the overall energy balance is lower, as shown in Fig. 9b: the share for the electrolysis subsection decreases from 95.37% to 78.36%.

4. Conclusions

A novel system for the production of green ammonia was designed and analysed. The introduction of high temperature electrolyser, such as SOE, permits to increase efficiency and system integration. The high efficiency of SOE permits electrical input reduction of the electrolyser unit and to recover heat produced in the Haber-Bosch reactor. The electricity consumption is decreased down to 8.30 kWh/kg NH_3 and zero emission of CO_2 is obtained. In the field of chemical production, the new system permits the production of zero emission ammonia and increases the flexibility of the plant compared to traditional electrolysers. Regarding this point, the stationary results reported here are encouraging for the further improvement of plant integration with other renewable energy systems, such as wind and solar systems connected to the SOE, in order to take into consideration power production variation and a dynamic modelling of the layout. Considering also the use of ammonia as a fuel and the energy storage application, a high efficiency and highly flexible concept is developed. Renewable electrical energy can be stored with an efficiency up to 62% into a liquid vector that can be transported and directly used both for power and transport applications.

The results assess the potential of a novel energy concept based on SOE as conversion technology and ammonia as fuel. NH_3 can be produced by distributed renewable energy sources directly on site. The chemical obtained is easily stored locally or transported and introduced in a more complex distribution system. In both cases it is possible to consider the final utilization in the transport sector, as a fuel, or in the power production sector for electrification with no emission of CO_2.

Appendix A

An advanced HB flowsheet has been drawn using AspenPlus Suite, according to the flowsheet of Fig. A1 below, and is always the same for each case.

The description of the parameters used in AspenPlus is as follows. The "MCompr" block type was used with the rigorous ASME method for efficiency, heat and power consumption calculation of the multistage compressor unit COMP01. Intercooling temperature after each stage and the final discharge pressure were specified for this block. EVA01 is modelled with a "HeatX" block type and the cold stream outlet temperature is fixed in order to exchange as much heat as possible. The specifications for the remaining blocks are summarized in Table A1.

The rigorous "RGibbs" reactor block is used to model the HBR with the Aspen built-in PENG-ROB method for physical and chemical equilibrium calculations. The vapour-liquid equilibrium flash drum model "Flash2" is the block used for SEP01, SEP02 and EXPANDER. The splitting ratio, i.e. the amount of purge gas, of the block SPLIT01 is used as convergence variable for the PFD. In order to increase the ammonia recovery from HBR product stream, the tail gas from EXPANDER and a part of the liquid ammonia produced are used to push the cooling of the feeding stream in EVA01. The cold stream coming out from this block, i.e. P-GAS, is gaseous NH_3 with some traces of inerts which can be still considered as useful product of the plant. The HB loop thus described produces ammonia both in liquid and gaseous forms.

The complete flowsheet of the reference case, NG-REF-HB is shown in Fig. A2.

Natural gas and air, at ambient temperature, are fed to an adiabatic combustor (BURNER), and a partial gasification process occurs with H_2 and CO formed together with CO_2. The N_2 necessary for NH_3 synthesis is fed in with the AIR stream. In the block REFORMER, a pre-heated steam stream is added to the burnt gas. The Steam-to-Carbon ratio (S/C) is fixed at 2 so that the Steam Methane Reforming (SMR) reaction can take place. Afterwards, three reactors are used (WGSR1, WGSR2, WGSR3) to complete the Water Gas Shift reaction (WGS). The reactions involved in these blocks are the following:

Table A1
Block specifications for the HB loop.

Specification	HBR	SEP01	SEP02	EXPANDER
Temperature (°C)	550	0	20	–
Pressure (bar)	250	250	250	1
Heat duty (kW)	–	–	–	0

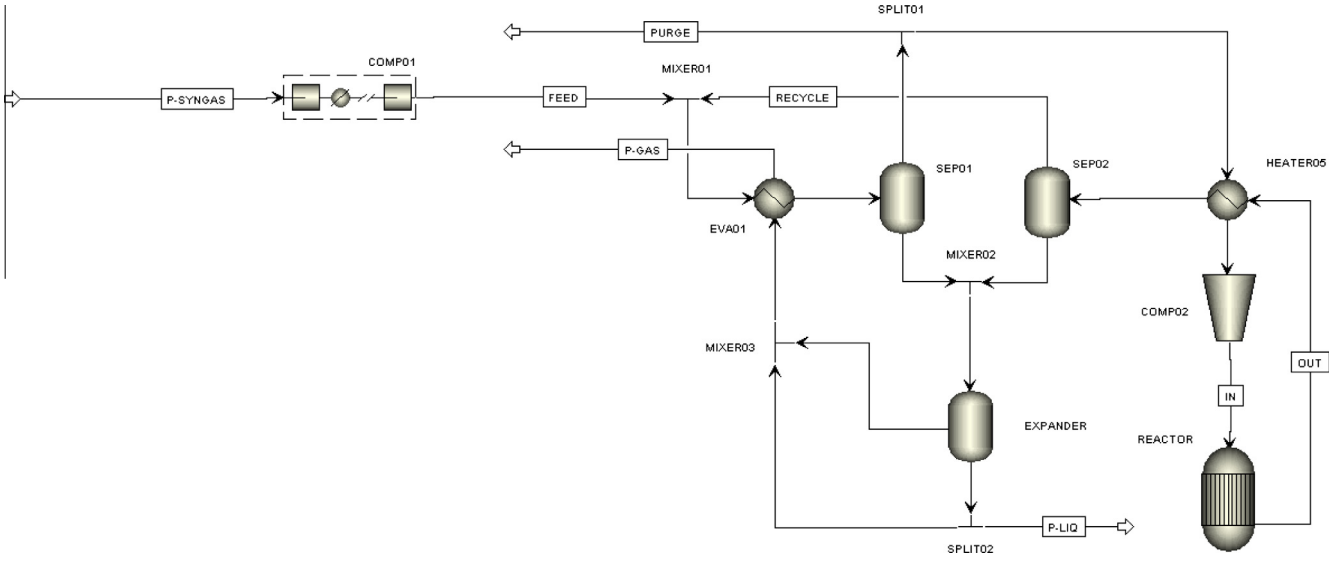

Fig. A1. Flowsheet of the HB loop developed in AspenPlus.

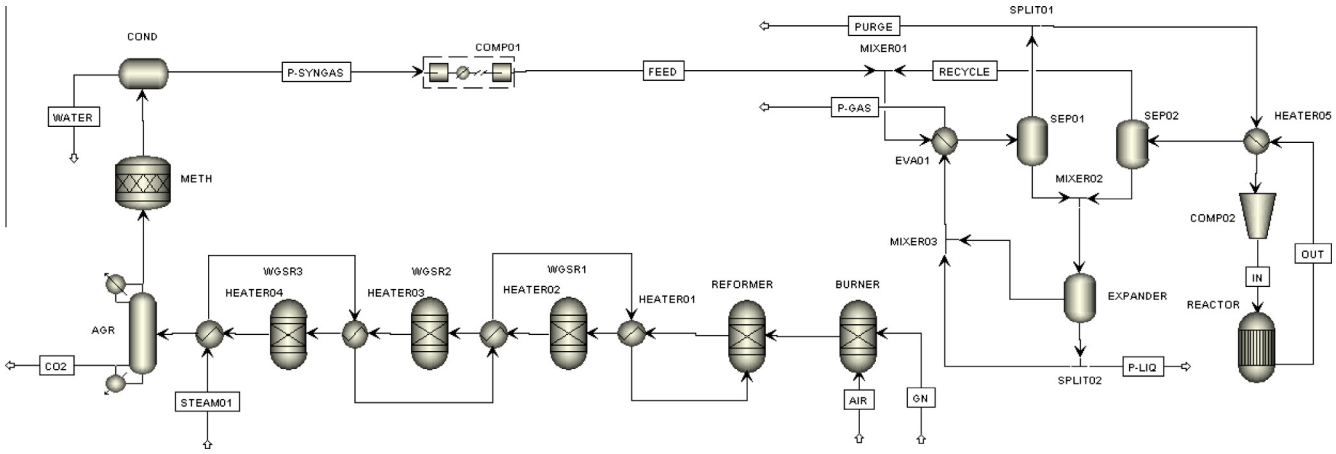

Fig. A2. Flowsheet diagram of the reference case NG-REF-HB.

$$CH_4 + H_2O = CO + 3H_2 \quad (A.1)$$

$$CH_4 + \frac{1}{2}O_2 = CO + 2H_2 \quad (A.2)$$

$$CO + H_2O = CO_2 + H_2 \quad (A.3)$$

$$CH_4 + 2O_2 = CO_2 + 2H_2O \quad (A.4)$$

The reactor block used to model all these units is "RGibbs" and the built-in NRTL Aspen property method was used for calculations. A "Sep" block with standard specifications concerning temperature (≈50–80 °C) and separation efficiency (>90%) is used for the AGR block [22]. An adiabatic "RStoic" reactor block is used by METH to convert residual CO_2 and COND is a "Flash2" block type, operated at 15 °C to allow and complete gas/liquid separation. Table A2 summarizes the specifications of those last three blocks.

Table A2
Block specifications for clean-up section.

Specification	AGR	METH	COND
Temperature (°C)	50	–	15
Pressure (bar)	1	1	1
Heat duty (kW)	–	0	–

The second case is named EL-PSA-HB and its schematic flow diagram is shown in Fig. A3.

The HB loop is the same as above, while the upstream architecture for low temperature electrolysis and PSA is simpler: water is compressed in a hydraulic pump (PUMP01) and heated in a counter current heat exchanger (HEATER01) to the electrolyser (ELECTR) operating conditions, namely 80 °C and 30 bar. The built-in "Pump" block has been used to model PUMP01, HEATER01 is a "HeatX" block type and ELECTR is an "RGibbs" reactor block. The electrochemical calculations for ELECTR block are based on commercial alkaline electrolysers data from literature [26]. The PSA standard process was modelled in Aspen Plus by means of a compressor (COMP03) and a separator (PSA) in series at 30 bar, room temperature and overall N_2 purity of 99.9% [23]. The property method used in this section was the NRTL built-in Aspen model.

Finally, the last case is the SOE-PSA-HB process illustrated in the flowsheet of Fig. A4.

In this case only, the ammonia reactor was forced to operate at 650 °C and 550 bar. In order to have comparable results with the

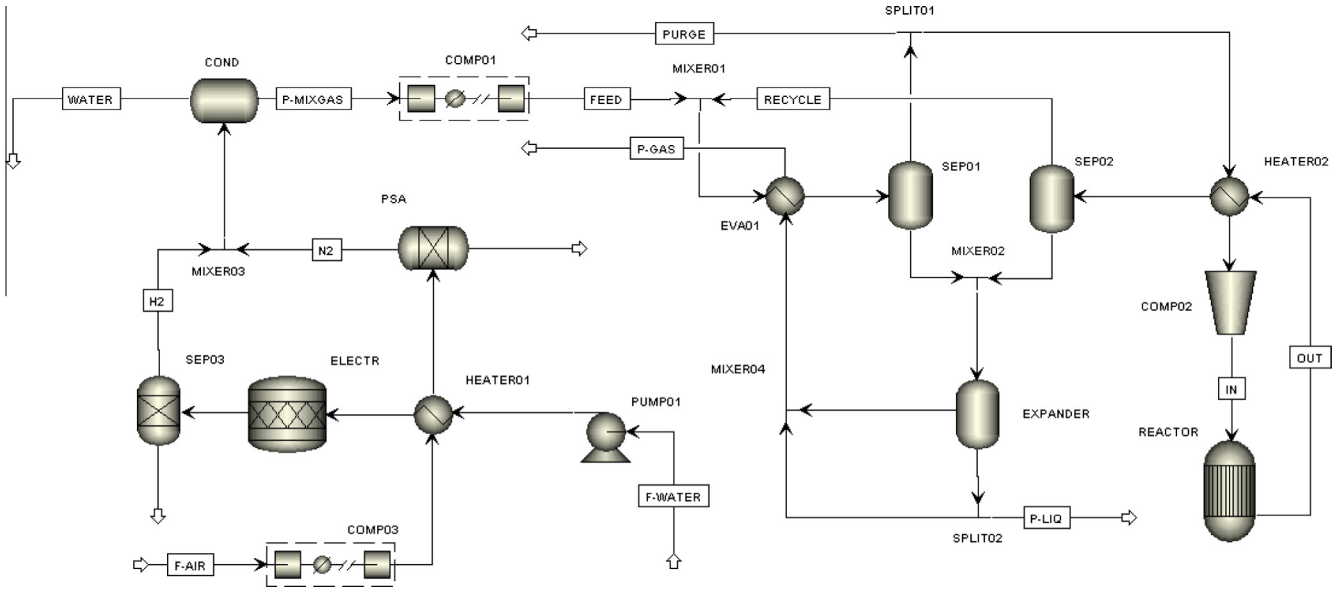

Fig. A3. Flowsheet diagram of the low temperature electrolysis case EL-PSA-HB.

Please cite this article in press as: Cinti G et al. Coupling Solid Oxide Electrolyser (SOE) and ammonia production plant. Appl Energy (2016), http://dx.doi.org/10.1016/j.apenergy.2016.09.026

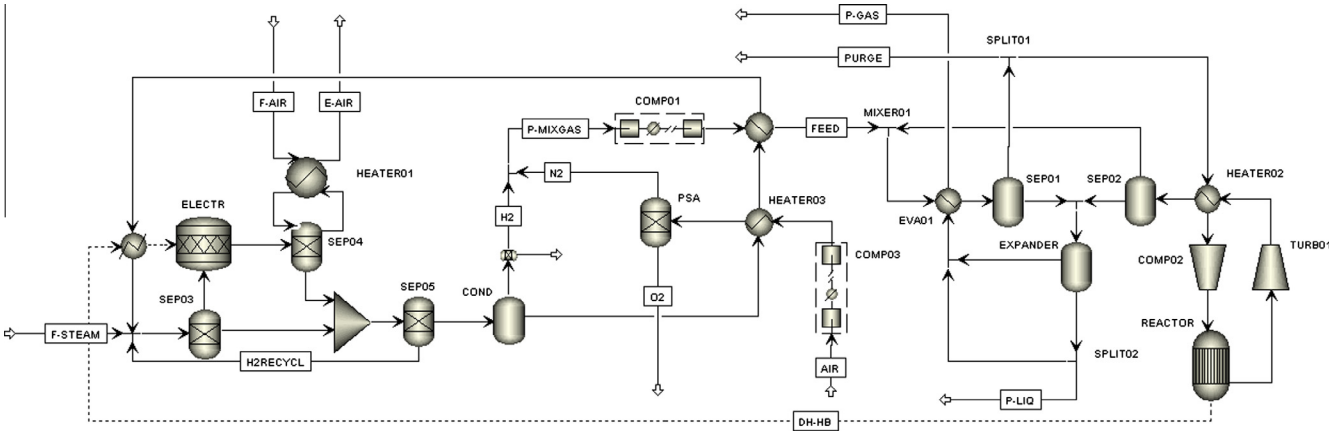

Fig. A4. Flowsheet diagram of the high temperature electrolysis case SOE-PSA-HB.

previous cases, the different pressure level is controlled only in the HB REACTOR block by using a pair of compressor/turbines before and after the block (COMP02, TURB01). Selected temperature and pressure are the highest that can be accepted for the HB process and, at the same time, this temperature is the lowest possible to consider in a SOE at the present stage of development. The original flowsheet representing the SOE unit [28] was here modified for the HB coupling purpose with the addition of a condenser (COND) to separate produced hydrogen (H2) from residual water, and a pre-heater at anode side (HEATER01), for preheating of the sweeping air (F-AIR) by heat recovery from oxygen enriched air (E-AIR) coming from anode outlet. The water separated from the COND block is used for cooling the feeding air of PSA block (AIR), and the feeding stream (FEED) before the HB loop. Afterwards, separated water is recycled to SOE as steam. Finally, the tear stream DH-HB represents the chemical heat available from the REACTOR block, due to ammonia reaction according to Eq. (1), that is used in SOE. The external subroutine for electrochemical calculations is based on the model described in Section 2.1, in order to consider the thermal contribution of HB coupling to the SOE energy balance. The only inputs to the subroutine are the operating temperature, already set at 650 °C, and the heat supplied to the SOE (DH-HB) per unit of hydrogen produced, to calculate k used in Eq. (10).

References

[1] Zamfirescu C, Dincer I. Ammonia as a green fuel and hydrogen source for vehicular applications. Fuel Process Technol 2009;90:729–37. http://dx.doi.org/10.1016/j.fuproc.2009.02.004.

[2] Frigo S, Gentili R. Analysis of the behaviour of a 4-stroke Si engine fuelled with ammonia and hydrogen. Int J Hydrogen Energy 2013;38:1607–15. http://dx.doi.org/10.1016/j.ijhydene.2012.10.114.

[3] Ryu K, Zacharakis-Jutz GE, Kong S-C. Effects of gaseous ammonia direct injection on performance characteristics of a spark-ignition engine. Appl Energy 2014;116:206–15. http://dx.doi.org/10.1016/j.apenergy.2013.11.067.

[4] Zamfirescu C, Dincer I. Using ammonia as a sustainable fuel. J Power Sources 2008;185:459–65. http://dx.doi.org/10.1016/j.jpowsour.2008.02.097.

[5] Comotti M, Frigo S. Hydrogen generation system for ammonia–hydrogen fuelled internal combustion engines. Int J Hydrogen Energy 2015;40:10673–86. http://dx.doi.org/10.1016/j.ijhydene.2015.06.080.

[6] Ferrero D, Lanzini A, Santarelli M, Leone P. A comparative assessment on hydrogen production from low- and high-temperature electrolysis. Int J Hydrogen Energy 2013;38:3523–36. http://dx.doi.org/10.1016/j.ijhydene.2013.01.065.

[7] Andersson J, Lundgren J. Techno-economic analysis of ammonia production via integrated biomass gasification. Appl Energy 2014;130:484–90. http://dx.doi.org/10.1016/j.apenergy.2014.02.029.

[8] Morgan E, Manwell J, McGowan J. Wind-powered ammonia fuel production for remote islands: a case study. Renew Energy 2014;72:51–61. http://dx.doi.org/10.1016/j.renene.2014.06.034.

[9] Patil A, Laumans L, Vrijenhoef H. Solar to ammonia – via proton's NFuel units. Proc Eng 2014;83:322–7. http://dx.doi.org/10.1016/j.proeng.2014.09.023.

[10] Giddey S, Badwal SPS, Kulkarni A. Review of electrochemical ammonia production technologies and materials. Int J Hydrogen Energy 2013;38:14576–94. http://dx.doi.org/10.1016/j.ijhydene.2013.09.054.

[11] Mingyi L, Bo Y, Jingming X, Jing C. Thermodynamic analysis of the efficiency of high-temperature steam electrolysis system for hydrogen production. J Power Sources 2008;177:493–9. http://dx.doi.org/10.1016/j.jpowsour.2007.11.019.

[12] Schulte Beerbühl S, Fröhling M, Schultmann F. Combined scheduling and capacity planning of electricity-based ammonia production to integrate renewable energies. Eur J Oper Res 2015;241:851–62. http://dx.doi.org/10.1016/j.ejor.2014.08.039.

[13] Frattini D, Cinti G, Bidini G, Desideri U, Cioff R, Jannelli E. A system approach in energy evaluation of different renewable energies sources integration in ammonia production plants. Renew Energ 2016;99:472–82.

[14] Laguna-Bercero MA. Recent advances in high temperature electrolysis using solid oxide fuel cells: a review. J Power Sources 2012;203:4–16. http://dx.doi.org/10.1016/j.jpowsour.2011.12.019.

[15] O'Brien JE, McKellar MG, Harvego EA, Stoots CM. High-temperature electrolysis for large-scale hydrogen and syngas production from nuclear energy – summary of system simulation and economic analyses. Int J Hydrogen Energy 2010;35:4808–19. http://dx.doi.org/10.1016/j.ijhydene.2009.09.009.

[16] Sanz-Bermejo J, Muñoz-Antón J, Gonzalez-Aguilar J, Romero M. Optimal integration of a solid-oxide electrolyser cell into a direct steam generation solar tower plant for zero-emission hydrogen production. Appl Energy 2014;131:238–47. http://dx.doi.org/10.1016/j.apenergy.2014.06.028.

[17] Cinti G, Baldinelli A, Di Michele A, Desideri U. Integration of Solid Oxide Electrolyzer and Fischer-Tropsch: a sustainable pathway for synthetic fuel. Appl Energy 2016;162:308–20. http://dx.doi.org/10.1016/j.apenergy.2015.10.053.

[18] Wendel CH, Braun RJ. Design and techno-economic analysis of high efficiency reversible solid oxide cell systems for distributed energy storage. Appl Energy 2016;172:118–31. http://dx.doi.org/10.1016/j.apenergy.2016.03.054.

[19] Tallaksen J, Bauer F, Hulteberg C, Reese M, Ahlgren S. Nitrogen fertilizers manufactured using wind power: greenhouse gas and energy balance of community-scale ammonia production. J Clean Prod 2015;107:626–35. http://dx.doi.org/10.1016/j.jclepro.2015.05.130.

[20] Appl M. Ammonia, principles and industrial practice. 1st ed. Weinheim: Wiley-Vch; 1999. http://dx.doi.org/10.1002/pauz.19970260615.

[21] Boudart M. Kinetics and mechanism of ammonia synthesis. Catal Rev 1981;23:1–15. http://dx.doi.org/10.1080/03602458108068066.

[22] Mondal P, Dang GS, Garg MO. Syngas production through gasification and cleanup for downstream applications — recent developments. Fuel Process Technol 2011;92:1395–410. http://dx.doi.org/10.1016/j.fuproc.2011.03.021.

[23] Ivanova S, Lewis R. Producing nitrogen via pressure swing adsorption. Chem Eng Prog 2012;108:38–42.

[24] Liso V, Nielsen MP, Kær SK. Influence of anodic gas recirculation on solid oxide fuel cells in a micro combined heat and power system. Sustain Energy Technol Assessments 2014;8:99–108. http://dx.doi.org/10.1016/j.seta.2014.08.002.

[25] Penchini D, Cinti G, Discepoli G, Desideri U. Theoretical study and performance evaluation of hydrogen production by 200 W solid oxide electrolyzer stack. Int J Hydrogen Energy 2014;39:9457–66. http://dx.doi.org/10.1016/j.ijhydene.2014.04.052.

[26] <www.fch.europa.eu/sites/default/files/study%20electrolyser_0-Logos_0_0.pdf> (last access 30/06/2016).

[27] <www.linde-engineering.com/internet.global.lindeengineering.global/en/images/HA_N_1_1_e_09_150dpi19_6131.pdf> (last access 30/06/2016).

[28] Cinti G, Discepoli G, Bidini G, Lanzini A, Santarelli M. Co-electrolysis of water and CO_2 in a solid oxide electrolyzer (SOE) stack. Int J Energy Res 2016;40:207–15. http://dx.doi.org/10.1002/er.3450.